Analytical Modeling of Losses for High Frequency Planar LCT Components

Kien Lai Dac, Yves Lembeye, Abdelhadi Besri, Jean-Pierre Kéradec

Analytical Modeling of Losses for High Frequency Planar LCT Components

Kien Lai-Dac, Yves Lembeye, Abdelhadi Besri and Jean-Pierre Keradec
G2Elab, UMR 5269-INPG-UJF-CNRS, BP46-38402- St Martin d'Hères Cedex - France
Kien.Lai-Dac@g2elab.grenoble-inp.fr

***Abstract* -- Passive components occupy a major part of the volume of power electronic converters. Therefore to increase the converter power density, designers have to carefully reduce the size of these components. The integrated planar inductor-capacitor-transformer, already known as LCT component can achieve this goal. Volume optimization of this component requires an accurate analytical modeling of overall losses (including magnetic, copper and the dielectric parts). However, common methods could not be used for high frequency planar components. In the first part of this paper, we introduce the principle and applications of LCT components. In the second part, we present an analytical electromagnetic and electrostatic modeling for high frequency planar components - the lumped elements equivalent circuit method. This method has been developed for components having simple geometries. The efficient application of this method to the complex geometry of LCT is showed in the third part.**

***Index Terms* – Integrated passive components, HF passive components, LCT components, planar components, losses modeling, LEEC method.**

I. NOMENCLATURE

LCT: Inductor-Capacitor-Transformer (component).
LEEC: Lumped Elements Equivalent Circuit (method).

II. INTRODUCTION OF LCT COMPONENT

The aim of this component is to gather three passive elements: inductor (L), capacitor (C) and transformer (T) into a unique mixed component. This device, called LCT, has many advantages because it enables a significant reduction in size and an improvement in performance by avoiding the interconnections needed to link three separated passive elements. Moreover, when built using planar technologies, this passive component set offers innovative integration techniques to be used for the design of power supplies.

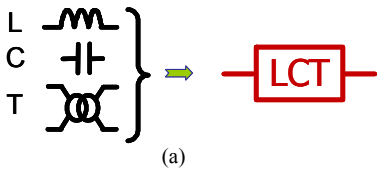

(a)

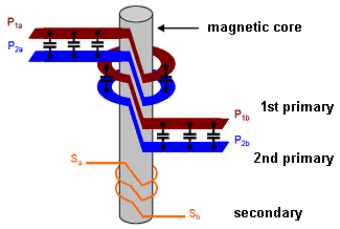

(b)

Fig.1. Principle of LCT components

The principle of a LCT is mainly that of a transformer (T). Splitting the primary winding in two, and intercalating a high permittivity dielectric material between the two primary layers, the capacitor function (C) is created. Leakage inductance of the transformer, controlled by an air gap in the side leg, gives the inductor function (L).

LCT components have various type of application. Firstly, by changing the wiring of its 4 primary points (P1a, P1b, P2a, P2b), it exhibits parallel or series resonance cell (fig.2). These cells are largely applied in many types of resonance converters (e.g. fig.3). The integrated capacitor in these type LCT components has a value around of some nF.

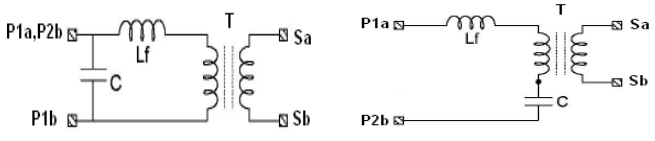

(a) (b)

Fig.2. Parallel and series resonance cells

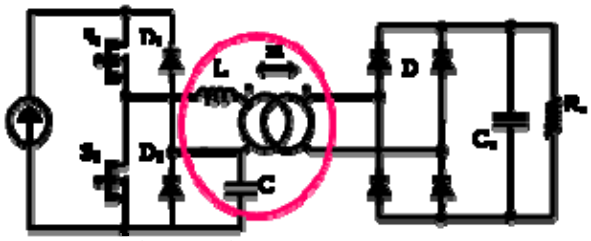

Fig.3. LCT in a resonant converter [5]

However, owing to the recent development of high permittivity dielectric material, the integrated capacitor can now reach higher values (from some tens nF to some µF).

These LCT components are able to be used in switch-mode power converters. Fig.4 presents a converter structure called Mixed Energy Transfer (MET) working in switch-mode [7].

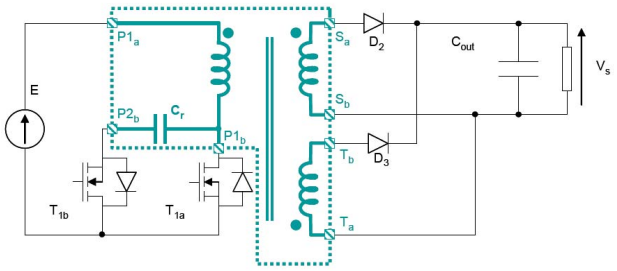

Fig.4. LCT in a switch-mode converter [7]

Several planar LCT have been built in our lab in the past [5]-[7]. We present here the prototype that will be used to model the losses in this paper (fig.5). Its double primary placed around the center leg of magnetic core owns twice 21 turns placed in twice 7 planar layers. These 14 coppers layers are separated by Pyralux®AP and Epoxy adhesive dielectric materials. One turn of Litz wire (*250 strands* of *100µm* diameter) is placed around one side core leg to form secondary winding and an air gap *1mm* thick is introduced in the other side leg. This LCT component has a leakage inductance of *115uH* and an integrated capacitance of *4.1nF*.

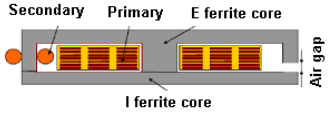

(b)

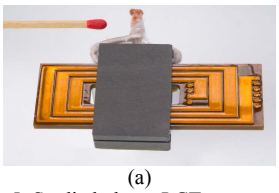

(a)

Fig.5. Studied planar LCT component

III. Introduction of LEEC Method

This modeling method applies to transformers that appear as a stack of conductive, insulating and magnetic plates. All plates are supposed infinite, made of materials assumed linear, homogeneous and isotropic so their electromagnetic properties are described by two scalars: complex permittivity and complex permeability. Energy transfer between conductive plates is due to electromagnetic propagation which is supposed unidirectional and normal to the layers.

This approach permits us to find a LEEC schematic that represents the electrical behavior of each layer of a planar component. Linking equivalent circuits of all plates fives the equivalent circuit for the whole component [4]. This LEEC model can be used to run frequency and time domain in circuit simulations.

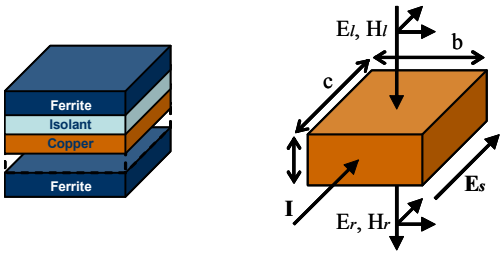

(a) (b)

Fig.6. Simplification hypothesis of LCCE method

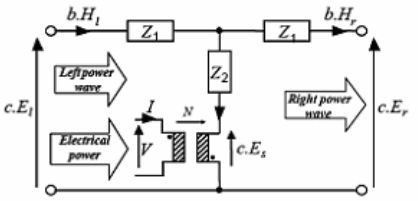

Fig.7. Equivalent physical circuit associated to a layer

Following this method, an elementary plate of a thickness "*a*", a width "*b*" and a length "*c*" is represented by an electrical equivalent circuit with impedances Z_1, Z_2 depending on the geometrical and physical nature of the layer.

TABLE I
EXPRESSION OF ELECTRIC COMPONENTS

$Z_c = \sqrt{\bar{\mu}/\bar{\varepsilon}}$	$\varphi = \omega\sqrt{\bar{\mu}\bar{\varepsilon}}\cdot a$	$A = e^{-j\varphi}$
$Z_1 = j.Z_c \cdot \frac{c}{b}\cdot\tan\left(\frac{\varphi}{2}\right)$	$Z_2 = j.Z_c.\frac{c}{b}\frac{1}{j\cdot\sin(\varphi)}$	

The LEEC schematics are deduced from these analytical expressions as follows. Dielectric and magnetic plate are not linked to external electrical circuit so the vertical part of the schematic is neglected and LEEC representation reduces to unique impedance equal to $2Z_1$. Then, from DC to a frequency of 10 times higher than plate thickness, convenient approximations apply to expressions show in Table.I. Accordingly, for a dielectric plate, the only impedance is an inductor.

$$L_a = \mu_0 \cdot \frac{ac}{b} \tag{1}$$

For a magnetic plate, same reason applies but expression (1) must include the complex relative permittivity μ_r (2) of ferrite material. In practice, frequency dependence of this impedance (which accounts for ferrite losses) is deduced (3) from impedance per square turn A_L and complex permeability available among manufacture data.

$$\bar{\mu}(f) = \mu_s'(f) - j.\mu_s''(f) \tag{2}$$

$$\overline{A_L}(f) = A_L \cdot \frac{\bar{\mu}(f)}{\bar{\mu}(0)} \tag{3}$$

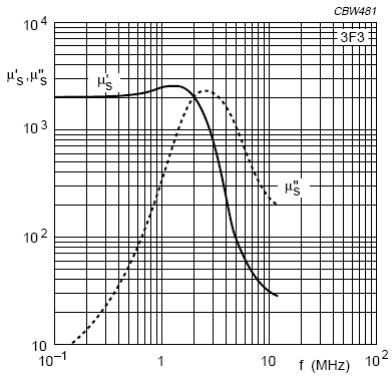

Fig.8. Permeability vs. frequency of ferrite 3F3®, as given by Ferroxcube™

From this expression, experimental approximations were applied to find its LEEC schematics. The larger the component number is, the more accurate model is. For our ferrite cores, a four element circuit (fig.9) supplies a representation accurate enough.

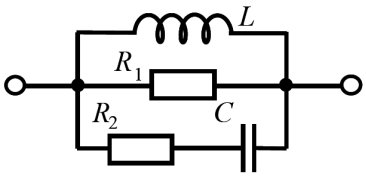

Fig.9. Core lumped element equivalent circuit

For conductive plates, LEEC representation is found [8], from analytical expressions given in Table.1, through two steps approach. First, circuit of fig.7 is changed to that of fig.10. In the later circuit, both impedances (A and B) own positive real parts so they are easier to represent by lumped elements. Second, circuits including minimum number of lumped elements (fig.11 and 12) are obtained to represent impedance A and B. Element values of related components are given in Table.II and III.

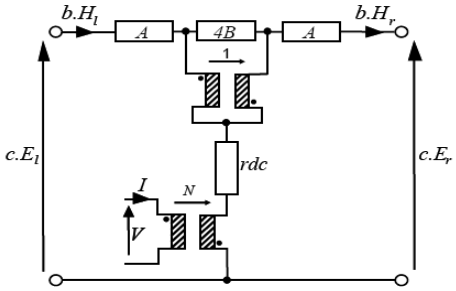

Fig.10. LEEC circuit for a conductive plate

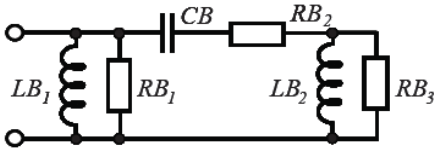

Fig.11. Lumped elements for impedance B

TABLE II

EXPRESSION OF COMPONENT VALUES FOR IMPEDANCE B BEFORE AND AFTER TUNING (2 LAST LINES)

Putting: $rdc = \frac{1}{\sigma}\frac{c}{ab}$ $ldc = \mu_0 \frac{ac}{b}$ $cdc = \mu_0.\sigma^2 \cdot \frac{a^3.b}{c}$		
$L_1 = \frac{1}{6} ldc$	$C = \frac{11}{1400} cdc$	$L_2 = \frac{25}{1782} ldc$
$R_1 = \frac{10}{7} rdc$	$R_2 = \frac{2380}{1089} rdc$	$R_3 = \frac{7865}{4869} rdc$
L_1 : *unchanged*	C : x .942	L_2 : x 2.44
R_1 : *unchanged*	R_2 : x .761	R_3 : x 1.303

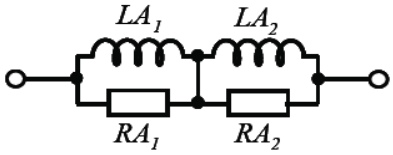

Fig.12. Lumped elements for impedance A

TABLE III
EXPRESSION OF COMPONENT VALUES FOR IMPEDANCE A

$LA_1 = 0.115\ ldc$	$LA_2 = 51.4\ 10^{-3}\ ldc$
$RA_1 = 4.93\ rdc$	$RA_2 = 15.92\ rdc$

Considering presented approach assumes energy transfer is due to electromagnetic waves normal to plates, electric field normal to the plates is not taken into account. For this reason, we now add another model to remedy this lack.

To compute the electrostatic field between two plates, we supposed that the potential of each conductive layer turn varies linearly when going from one terminal to the other. In this condition, the electric field in the dielectric layer is easily deduced and so it is for the electrostatic energy stored in that volume. Finally, a set of 6 capacitors is used to represent the capacitive coupling between two conductive layers (fig.13), in which the capacitance C_0 is obtained when there is no direct electrical connection between the two conductive layers.

$$C_0 = \varepsilon_0.\varepsilon_r \cdot \frac{b.c}{a} \qquad (4)$$

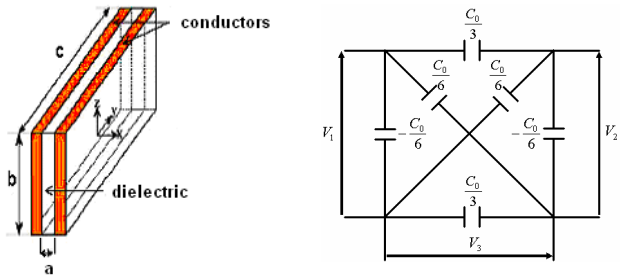

(a) (b)
Fig.13. Equivalent circuit for inter-layer capacitances

Finally, special attention must be paid to series capacitor (part C of LCT). This capacitor is made of Kapton®AP Pyralux and Epoxy adhesive which show losses that cannot be neglected (fig.14). The procedure to reach LEEC schematic is similar to the magnetic losses model. Notice that, the complex permittivity of dielectric material using in the LCT prototype is not given by manufacturer. So we only use loss tangent coefficient to determine the equivalent series resistance (ESR) of the integrated capacitor.

$$ESR(f) = \frac{\tan\delta}{2.\pi.f.C} \quad (5)$$

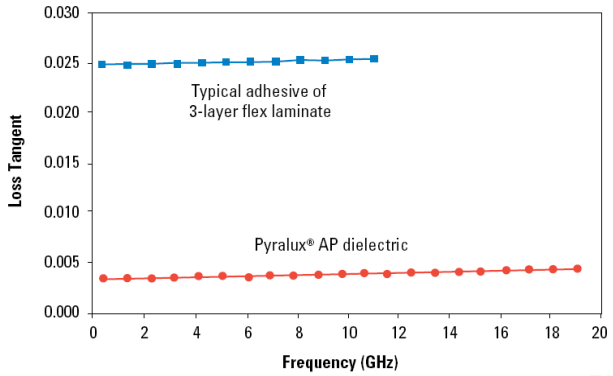

Fig.14. Loss tangent of Pyralux®AP and adhesive, as given by Dupont™

In order to find the LEEC schematic from analytical expression (5), we used the three RC cells in parallel and connect them in parallel to the capacitor (fig.15). One more time, the higher number of RC cells is, the more accurate dielectric loss model is. But in practice, to reach an inaccuracy equal or lower than 1% over a wide frequency range, only three cells are required for the model.

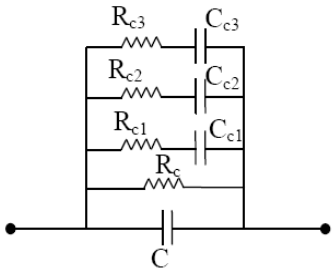

Fig.15. Equivalent circuit for dielectric losses

When all types of plates (magnetic, conductor, dielectric) are represented by their corresponding LEEC schematics, the combination of overall parts is implemented in a circuit simulator such as PSpicec®, PSIM®,… to study the frequency domain behavior. Owning to the lumped element nature of the circuit, time domain behavior of a complete circuit including this component is also possible. At the end, losses of different types (ferrite, copper or dielectric) are deduced from these simulations.

It would be advisable to talk about the method limitations. Firstly, this method is based on the assumption of a 1D propagation of the electromagnetic wave through parallel layers. To respect the simplifying assumptions, the component geometry must look like a stack of plane layers or different materials which are homogenous and isotropic.

However, due to the weak relative curvature of their layers, some transformers owning cylindrical winding can be modeled this way. Sometimes also, the component can be split into several parts which, individually, satisfy geometry requirements. LEEC associated to the whole component can be drawn by linking LEEC related to each part.

Secondary, another limitation of LEEC method is due to the imperfections of manufacture data related to the magnetic and dielectric loss. For example, the complex permeability of magnetic core material (including its imaginary part) is given by manufacturer over a bounded frequency range (from 10kHz up to 10MHz). For dielectric loss of numerous materials, the situation is worst. Complex permittivity is so difficult to measure that manufacturer do not provide any data about it. More over, even when these data are supplied, they are always accompanied by an uncertainty due to the manufacturing dispersion.

Finally, the LEEC model of magnetic and dielectric depends essential to the experience approximation procedures.

IV. Application of LEEC Method in Modeling of Losses of LCT Planar Components

As we can see at the transversal view of the studied LCT (fig.16), its geometry is quite asymmetric. In order to apply the LEEC method to the particular geometry of LCT components, we have transformed the topological shape of the core to an imaginary equivalent symmetrical form. By using hypothesis that electromagnetic waves transfer from plate to plate of the primary and pass to the secondary through the two leakage drains placed between the two windings, the electromagnetic phenomena is identical in both real and imaginary conceptions. This assumption will be verified by obtained accurate results.

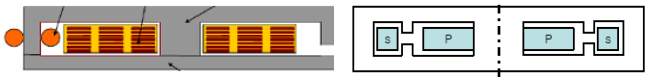

(a) (b)

Fig.16. Real (a) and imaginary (b) conception of studied LCT

We can determine an analytical expression for the leakage inductance. It is deduced from the size of the air gap and the windings. By assuming that the major part of leakage energy is stored in the air gap, the leakage inductance is calculated in (6), where N is the number of primary winding turns, A_e and e are the section and the thickness of the air gap.

$$L_f = \frac{\mu_0.N^2.A_e}{e} \quad (6)$$

In benefit of the symmetric representation, the LEEC method can be applied to the LCT components. The core is modeled by two identical RLC cells, each one represents a

half of the core. A neutral common point has to be placed between these two cells in respect to the electric field reference of overall LEEC schematic. We neglected the impact of the air gap on the current density distribution in the windings. In fact, this influence is small if the winding is well far separated from the gap. The leakage is represented by an inductor.

We focus now on the planar primary layers. The studied LCT component has two different widths on the primary winding tracks, a thin slip of *1.5mm* width and a larger one of *3.5mm* width (fig.17). To simplify the model, we transferred them to an average width b_{prim} and an average length c_{prim} by keeping the copper surface.

$$c_{prim} = \frac{\Sigma c_i}{n_{turn}} \tag{7}$$

$$b_{prim} = \frac{\Sigma b_i . c_i}{n_{turn} . c_{prim}} \tag{8}$$

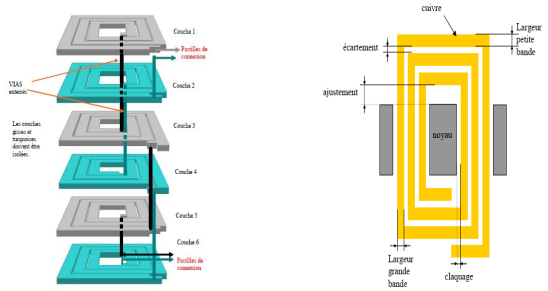

(a) (b)

Fig.17. Geometry of studied LCT planar primary layers

For the secondary Litz winding of one turn, we homogenize its N strands to a square solid plate.

$$a_{sec} = b_{sec} = \sqrt{\pi . N_{trands}} \frac{d_{strands}}{2} \tag{9}$$

Focusing to the dielectric coupling, it's is important to notice that the modeling of the separated turns on each layers taking into account the position of interlayer connections is the key to obtain more accurately and close to the measurement. A LEEC representation of three separate turns for each layer of primary winding has more accurate electrostatic behavior than a LEEC representation of whole 3 turns in one layer.

When the LEEC schematics of all layers are described and the model has been implemented in PSpice®, PSIM® simulators. Each layer was regrouped in a bloc. The global schematic seems to be complex but many of blocs are identical because the physic associated layers in the planar components are quite the same. The iterative procedure can reduce the complexity of model design.

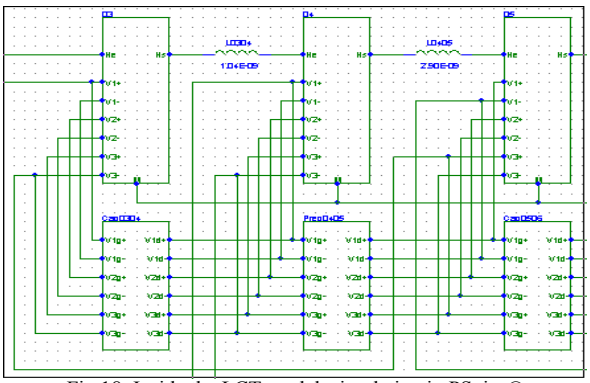

Fig.18. Inside the LCT model, simulation in PSpice®

To validate the designed model, frequency domain and time domain simulations were carried out and compared with measurement. It would be better to cut down as short as possible the connections from LCT component to converter card and to the measurement devices because they evidently have influences on the measurement accuracies.

We firstly measured impedances of this prototype by the impedance analyzer "Agilent 4294A" and compared with the simulated impedance. The frequency range is wide (from 40Hz to 110Mhz). The results show that the impedances (in general the electromagnetic and electrostatic behavior) were accurately modeled up to very high frequency (fig.19-22).

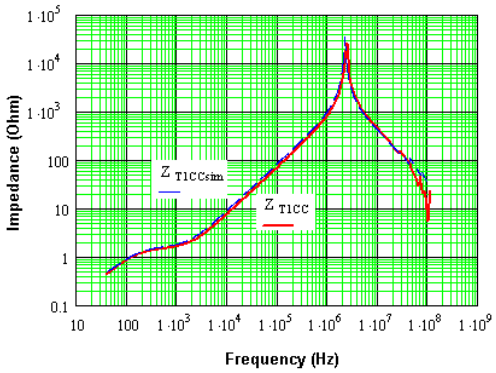

Fig.19. Primary impedance (P1a-P1b), short-circuit at secondary – simulation (dot blue line) vs. measurement (solid red line)

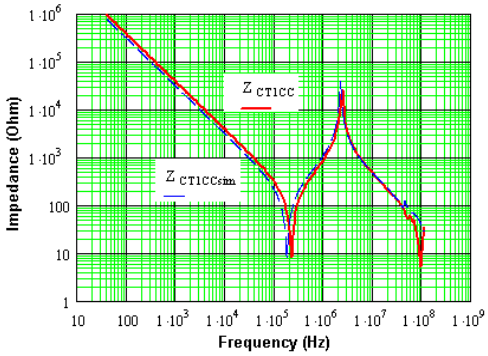

Fig.20. Primary impedance (P1a-P2b), short-circuit at secondary – simulation (dot blue line) vs. measurement (solid red line)

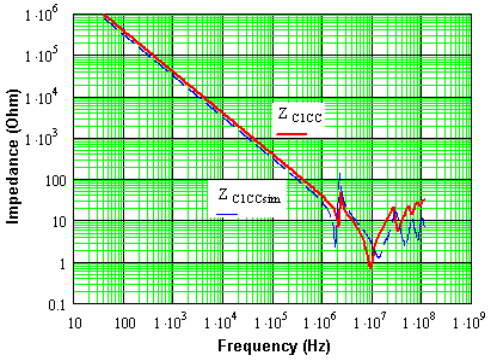

Fig.21. Primary impedance (P1b-P2b), short-circuit in secondary – simulation (dot blue line) vs. measurement (solid red line)

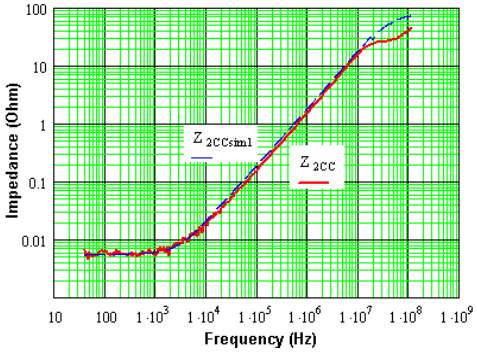

Fig.22. Secondary impedance, short-circuit at primary (P1a-P1b) – simulation (dot blue line) vs. measurement (solid red line)

To validate the time domain simulation, this component is placed into a quasi resonant half bridge DC-DC converter (input: power *60W,* DC input voltage *300V*, DC output voltage *5V*, switching frequency *180 kHz*). We used PSIM® simulator to eliminate the convergence problem due to large number of elements in LCT model. These accurate results (fig.24-28) permit us to use this method in modeling of losses for LCT components.

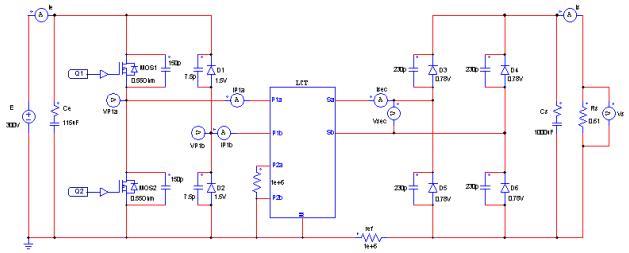

Fig.23. LCT model in a DC-DC, simulation in PSIM®

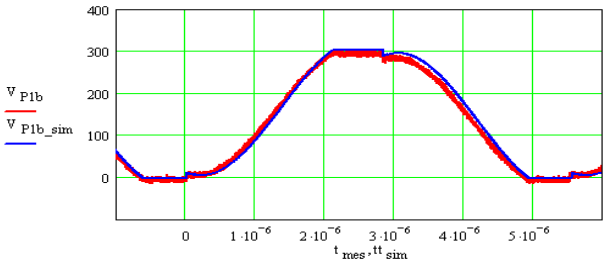

Fig.24. Tension at P1b: simulation (blue line) vs. measurement (red line)

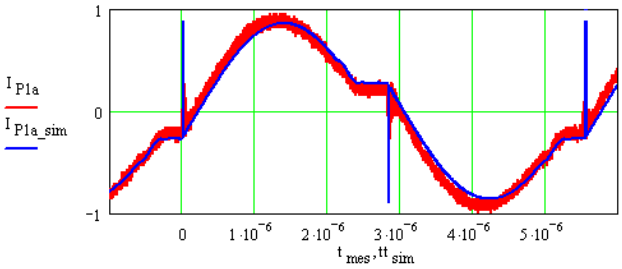

Fig.25. Current at P1a: simulation (blue line) vs. measurement (red line)

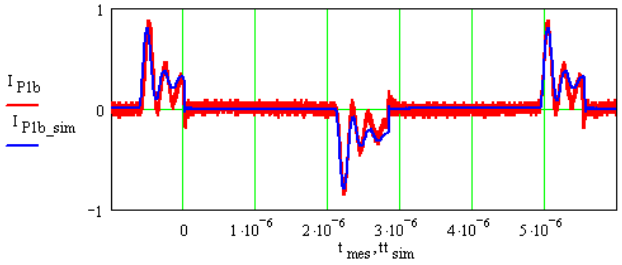

Fig.26. Current at P1b: simulation (blue line) vs. measurement (red line)

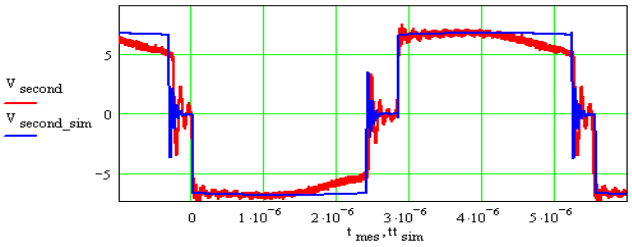

Fig.27. Tension Sa-Sb: simulation (blue line) vs. measurement (red line)

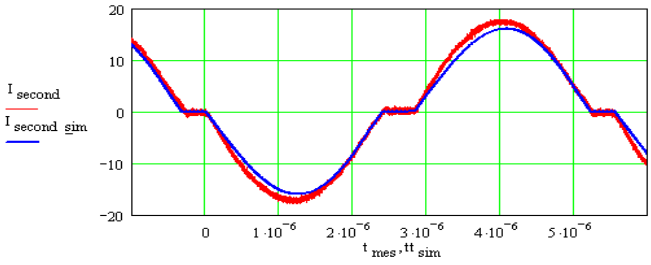

Fig.28. Current at secondary of LCT: simulation (blue line) vs. measurement (red line)

The losses in LCT are deduced from the dissipated power in the resistance elements of all component layers. For the planar primary part of LCT component, it is not possible to calculate for all layers due to limitation of informatics' resources. Therefore, one represent layer is used to estimate losses, all others similar layers are supposed having the same losses. Thanks to the modelling, we can separate these losses natures in three groups of materials (ferrite, copper and dielectric). We present the losses simulated which are suitable with the measurement at the table IV. We can also determine the different nature of losses (DC losses and eddy current losses) in copper winding (table V). The DC loss in a conductive layer is the power dissipated by r_{dc} and the losses due to eddy current are losses in A and B impedances in fig.10.

TABLE IV
LOSSES CALCULATION OF LCT: SIMULATION VS. MEASUREMENT

LCT losses (W)	Copper	Ferrite	Dielectric	Total
Simulation	1.895	1.382	0.454	**3.731**
Measurement				**3.92**

TABLE V
SEPARATION OF COPPER LOSSES IN LCT THANKS TO SIMULATION

Copper losses (W)	DC	Eddy current	Total
Primary	0.17	0.016	0.186
Secondary	1.223	0.486	1.709
Total	1.393	0.502	**1.895**

There are some interesting results to point out. In the first instance, the majority of cooper loss is in the secondary winding. In reality, we could reduce the DC losses of this winding by using more Litz wire strands in parallel, but it would possible increase the eddy current losses due to the proximity effect. Moreover, the eddy current losses in secondary winding should be discussed because we had homogenized this wire to a square solid plate, the skin effect was not exactly modeled and this loss simulated is possible higher than in actual fact. It could be better modeled if we had homogenized it to many plates whose thickness is equal to the diameter strand of Litz wire. But the modelling by such model for only one turn secondary seemed to be too complex. In the second instance, the low losses in planar primary in comparison with classical secondary winding signify the advantage of the planar technology for the integration of passive component.

V. CONCLUSION

The planar integrated passive component LCT has been studied for many years and its applications are widely increasing and interesting for industry. The optimization of these components is a necessary need so that warrants further researches. This study has shown an accurate analytical modeling of electromagnetic and electrostatic behavior in planar LCT components by the LEEC method. Based on these results, since the model is fully analytical, the losses calculations will have be directly estimated and linked to the device geometry and physics. This model of losses will be integrated with an analytical thermal model in order to perform optimization and sizing routines. It permits us to design better the LCT components, thereby to achieve more controls in their fabrication.

REFERENCES

[1] M. C. Smit, J. A. Ferreira, and J. D. Van Wyk, "A planar integrated resonant L–C–T circuit using ceramic dielectric and magnetic material," in Proceeding of IEEE Industry Applications Conf., vol. 2, 1994, pp. 1233–1249.

[2] I. W. Hofsajer, J. A. Ferreira, and J. D. Van Wyk, "Optimized planar integrated L–C–T components," in Proceeding of IEEE PESC'97 Conf., vol. 2, 1997, pp. 1157–1163.

[3] I. W. Hofsajer, J. A. Ferreira, and J. D. Van Wyk, "Design and analysis of planar integrated L–C–T components for converter," IEEE Transaction on Power Electron., vol. 15, no. 6, pp. 1221–1227, Nov. 2000.

[4] A. Schellmanns, P. Fouassier, J-P. Keradec, J-L. Schanen, "Equivalent Circuits for Transformers Based on One-Dimensional Propagation: Accounting for Multilayer Structure of Windings and Ferrite Losses", IEEE Transactions on Magnetics, Vol. 35, No. 5, September 2000.

[5] K. Laouamri, J.-P. Keradec, J.-P. Ferrieux, and S. Catellani, "Design and identification of an equivalent circuit for L–C–T component: inventory and representation of losses," in Proceeding of IEEE Instrumentation Measurement Technology Conf., vol. 2, 2003, pp. 1061–1066.

[6] Y.Lembeye, P.Goubier and J.P Ferrieux "Intergrated planar LCT component: Design, Characterization and Experimental Efficiency Analysis", IEEE Transaction on Power Electronic, Vol. 20, No. 3, May 2005.

[7] B. Vallet, Y.Lembeye, J.P; Ferrieux, "Mixed energy transfer (MET) innovative structure based on LCT and comparison with traditional structures". Conference Record of the 2006 IEEE Industry Applications Conference Forty First IAS Annual Meeting IEEE Cat.-No.-06CH37801. 2006: 8 pp. vol.4

[8] A. Besri, X.Margueron, J.P. Keradec, B. Declinchant, "Wide Frequency Range Lumped Element Equivalent Circuit for HF Planar Transformer", in Proceeding of IEEE, PESC-2008